We are IntechOpen, the world's leading publisher of Open Access books Built by scientists, for scientists

4,800
Open access books available

122,000
International authors and editors

135M
Downloads

Our authors are among the

154
Countries delivered to

TOP 1%
most cited scientists

12.2%
Contributors from top 500 universities

CLARIVATE ANALYTICS BOOK CITATION INDEX INDEXED

WEB OF SCIENCE™

Selection of our books indexed in the Book Citation Index in Web of Science™ Core Collection (BKCI)

Interested in publishing with us?
Contact book.department@intechopen.com

Numbers displayed above are based on latest data collected.
For more information visit www.intechopen.com

Chapter 8

Surface Functionalization of Graphene with Polymers for Enhanced Properties

Wenge Zheng, Bin Shen and Wentao Zhai

Additional information is available at the end of the chapter

http://dx.doi.org/10.5772/50490

1. Introduction

Graphene, a single-atom-thick sheet of hexagonally arrayed sp^2 bonded carbon atoms, has been under the spotlight owning to its intriguing and unparalleled physical properties [1]. Because of its novel properties, such as exceptional thermal conductivity, [2] high Young's modulus, [3] and high electrical conductivity,[4] graphene has been highlighted in fabricating various micro-electrical devices, batteries, supercapacitors, and composites [5, 7]. Especially, integration of graphene and its derivations into polymer has been highlighted, from the point views of both the spectacular improvement in mechanical, electrical properties, and the low cost of graphite [8, 9]. Control of the size, shape and surface chemistry of the reinforcement materials is essential in the development of materials that can be used to produce devices, sensors and actuators based on the modulation of functional properties. The maximum improvements in final properties can be achieved when graphene is homogeneously dispersed in the matrix and the external load is efficiently transferred through strong filler/polymer interfacial interactions, extensively reported in the case of other nanofillers. However, the large surface area of graphene and strong van der Waals force among them result in severe aggregation in the composites matrix. Furthermore, the carbon atoms on the graphene are chemically stable because of the aromatic nature of the bond. As a result, the reinforcing graphene are inert and can interact with the surrounding matrix mainly through van der Waals interactions, unable to provide an efficient load transfer across the graphene/matrix interface. To obtain satisfied performance of the final graphene/polymer composites, the issues of the strong interfacial adhesion between graphene–matrix and well dispersion of graphene should be addressed.

To date, the mixing of graphene and functionalized graphene with polymers covers the most of the published studies, and the direct modification of graphene with polymers is a

somewhat less explored approach. However, in many cases, to achieve stable dispersions of graphene and adequate control of the microstructure of the nanocomposites, non-covalent or covalent functionalization of graphene with polymers may be necessary. The non-covalent functionalization, which relies on the van der Waals force, electrostatic interaction or π-π stacking [10, 12], is easier to carry out without altering the chemical structure of the graphene sheets, and provides effective means to tailor the electronic/optical property and solubility of the nanosheets [13]. The covalent functionalization of graphene derivatives is mainly based on the reaction between the functional groups of the molecules and the oxygenated groups on graphene oxide (GO) or reduced GO (r-GO) surfaces [14, 15], such as epoxides and hydroxyls on their basal planes and carboxyls on the edges [16]. Compared with non-covalent functionalization, the covalent functionalization of graphene-based sheets holds versatile possibility due to the rich surface chemistry of GO/r-GO. However, it should be pointed out that the non-covalent or covalent attachment of graphene to polymer chains can improve some properties, but may be negative for others, especially those related to the movement of electrons or phonons. Although the functionalization of graphene with polymers is generally attempted with a view to conferring to the polymer new or improved properties, the polymer may also prevent the aggregation of the graphene sheets, where the graphene-polymer size ratio and molecular weight play important roles. For general bibliography on typical graphene-based nanocomposites, the reader can consult several monographs, reviews, and feature articles that summarize the state of the art of the field.

The objective of the present work is to provide a broad overview on the methods developed to non-covalently or covalently bind graphene to polymers. The covalent linking of polymeric chains to graphene is at its initial stages and there is significant room for the development of new and improved strategies.

2. The precursor of functionalized graphene

As we know, GO is the main precursor for the functionalization of graphene with polymers. It is because that there are multiple oxygen-containing functionalities, such as hydroxyl, epoxy and carboxyl groups on GO sheets [16]. GO is usually produced using different variations of the Staudenmaier [17] or Hummers [18] method in which graphite is oxidized using strong oxidants such as $KMnO_4$, $KClO_3$, and $NaNO_2$ in the presence of nitric acid or its mixture with sulfuric [19, 20]. For more details about GO, we refer the reader to the extensive review of GO preparation, structure, and reactivity by Dreyer et al and Zhu et al. [19, 20].

Furthermore, the reduction of GO will remove most, but not all, of the oxygen-containing functionalities such as hydroxyl, carboxylic acid and epoxy groups. Therefore, some functionalization reactions are based on the reduced GO. Generally, GO can be exfoliated using a variety of methods, most commonly by solvent-based exfoliation and reduction in appropriate media or thermal exfoliation and reduction [16, 21] In the former route, the hydrophilic nature and increased interlayer spacing of GO facilitates direct exfoliation into solvents

http://dx.doi.org/10.5772/50490

(water, alcohol, and other protic solvents) assisted by mechanical exfoliation, such as ultrasonication and/or stirring, forming colloidal suspensions of "graphene oxide". The chemically reduced graphene oxide is produced by chemical reduction of the exfoliated graphene oxide sheets using hydrazine, [22, 24] dimethylhydrazine, [25] sodium borohydride followed by hydrazine, [26] hydroquinone, [27] vitamin C, [28] etc. However, the hazardous nature and cost of the chemicals used in reduction may limit its application. The most promising methods for large scale production of graphene is the thermal exfoliation and reduction of GO. Thermally reduced graphene oxide can be produced by rapid heating of dry GO under inert gas and high temperature [29, 31]. Heating GO in an inert environment at 1050°C for 30 s leads to reduction and exfoliation of GO, producing low-bulk-density TRG sheets, which are highly wrinkled [32]. In the thermal process, the epoxy and hydroxyl sites of GO decompose to produce gases like H_2O and CO_2, yielding pressures that exceed van der Waals forces holding the graphene sheets together, causing the occurrence of exfoliation.

3. Covalent functionalization of graphene with polymers

It is desirable that stronger bonds are usually formed between the graphene and the polymers by covalent functionalization of graphene with polymers. However, it is usually difficult to realize because ideal graphene lacks functional groups that can be conjugated with. In some cases, when the graphene sheets were exfiolated from GO, incomplete reduction process leaves oxygen-containing functionalities that are then available for further functionalizations. Other covalent functionalization strategies typically involve further disruption of the conjugation of the graphene sheets. Although covalent functionalization of graphene will compromise some of its natural conductivity, this method is still valuable in some cases when graphene's other properties are desirable. More details of graphene functionalization via covalent bonds will be discussed below.

3.1. Functionalizations via "grafting from" method

Until now, "grafting to" and "grafting from" techniques have been developed to graft the polymer chains onto the graphene surface. The "grafting from" method relies on the immobilization of initiators at the surface of graphene, followed by in situ surface-initiated polymerization to generate tethered polymer chains. A number of studies of polymer-functionalized graphene by the "grafting from" method have been reported.

3.1.1. Atom transfer radical polymerization (ATRP)

Among the types of "grafting from" polymerization [33, 46], ATRP is the most widely used, and represents the majority of the studies reported. ATRP is almost certainly chosen because it offers the advantages of radical polymerization, that is, a fast initiation process and the development of a dynamic equilibrium between dormant and growing radicals [47]. In addition, a wide range of monomers can be polymerized by ATRP with controlled chain length. Moreover, block copolymers can be prepared by ATRP because of the living radical

process. Furthermore, ATRP is probably the most practical technique for preparation of functional polymers because the terminal alkyl halide can be converted to a wide variety of functionalities by using conventional organic synthetic procedures.

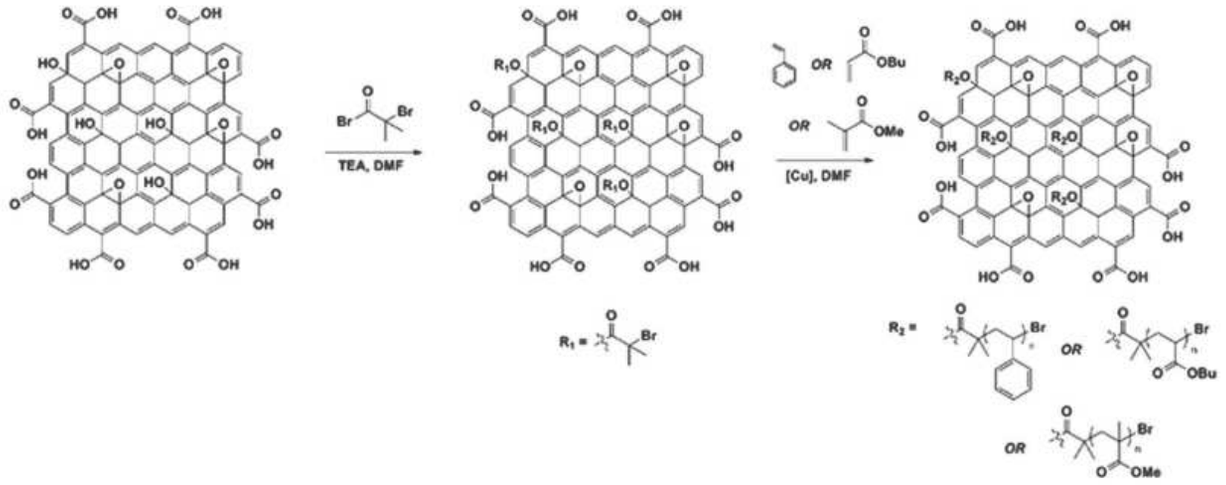

Figure 1. Synthesis of surface-functionalized GO via attachment of an ATRP initiator (a-bromoisobutyryl bromide) followed by polymerization of styrene, butyl acrylate, or methyl methacrylate [38].

Lee et al. [38] have reported a new method for attaching polymer brushes to GO sheet using surface-initiated ATRP. The hydroxyl groups present on the surface of GO were first functionalized with a wellknown ATRP initiator (a-bromoisobutyryl bromide), and then polymers of styrene, butyl acrylate, or methyl methacrylate were grown directly via a surface-initiated polymerization (SIP) (Figure 1). The authors studied the case of polystyrene (PS) in detail and presented two main conclusions. First, they suggested that the polymer chain length can be tunable by changing the ratio of monomer and initiator modified GO. Second, they reported that the monomer loading can vary the molecular weight of the grafted PS, which was obtained by gel permeation chromatography (GPC) after detaching by saponification, and the polydispersity was low, which suggested the polymerization proceeds in a controlled manner. Furthermore, the PS-functionalized GO was shown to significantly increase the solubility in N,N-dimethylformamide (DMF), toluene, chloroform, and dichloromethane, improving the processing potential of these materials for applications in polymer composites.

Fang et al. [43, 44] demonstrated the ability to systematically tune the grafting density and chain length of PS covalently bonded to graphene sheets by combining diazonium addition and ATRP. After reduction, r-GO was functionalized with 2-(4-aminophenyl) ethanol, reacted with 2-bromo-2-methylpropi-onyl bromide (BMPB), and subsequently the polymerization of styrene was carried out (Figure 2). Their results showed that the polydispersity of the high grafting density sample was more uniform than that of the low grafting density, which was attributed to the the degree of functionalization of r-GO sheets with the initiator because the diazonium coupling to graphene follows an identical radi-

http://dx.doi.org/10.5772/50490

cal mechanism as that for carbon nanotubes (CNTs). The relaxation of the polymer chains covalently bonded to the r-GO surface was strongly confined, particularly for segments in close proximity to the r-GO surface. This confinement effect could enhance the thermal conductivity of the polymer nanocomposites. The significant increases in thermal conductivity were observed for only 2.0 wt% functionalized r-GO in PS composites. Also, the resulting PS nanocomposites with 0.9 wt% functionalized r-GO revealed around 70% and 57% increases in tensile strength and Young's modulus.

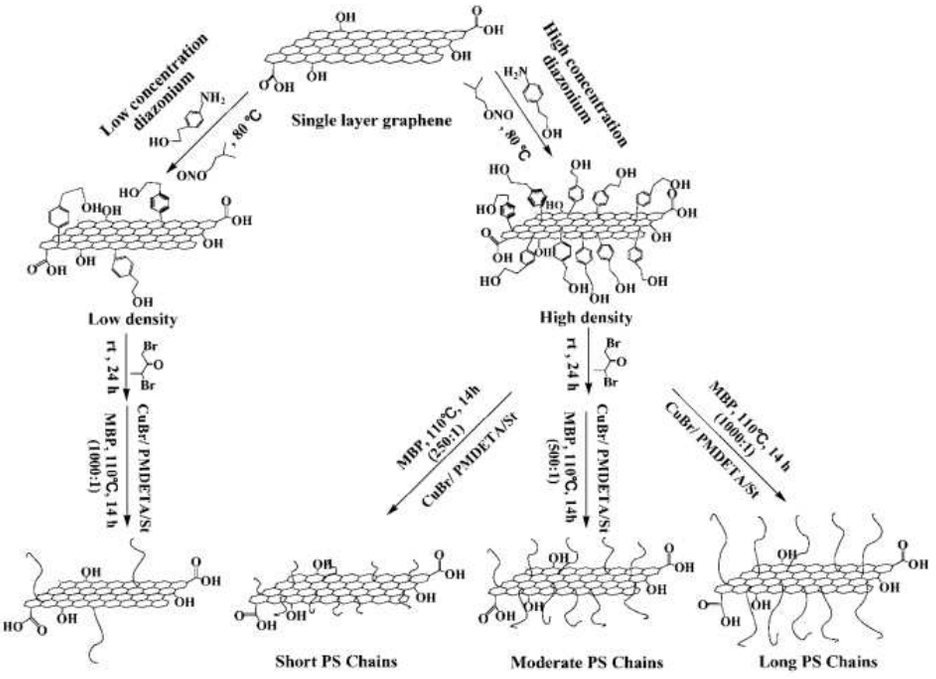

Figure 2. Synthetic routes for achieving controllable functionalization of graphene.[28]

Furthermore, Gonçalves et al. [40] developed the use of poly(methyl methacrylate) (PMMA) grafted from carboxylic groups in GO as a reinforcement filler. Here the BMPB initiators were immobilized by two esterification reactions: the carboxylic groups of GO were esterified with ethylene glycol, followed by reacting with BMPB using the same type of reaction as Lee et al. [38]. In this case, the polydispersity of the grafted PMMA, removed from the GO by hydrolysis, was found to be close to unity, once more suggesting a well-controlled process irrespective of the under estimated molecular weights. This PMMA-functionalized GO showed a good solubility in organic solvents such as chloroform and could be used as reinforcement filler in the preparation of PMMA composite films. Due to the strong interfacial interactions between the PMMA-functionalized GO and PMMA matrix caused by the presence of short PMMA chains covalently bonded to GO, an efficient load transfer from the GO to the matrix was formed, thus improving the mechanical properties of their nanocomposites, which were more stable and tougher than pure PMMA and its nanocomposites with unmodified GO (Figure 3). For example, addition of 1 wt% PMMA-functionalized GO clearly led to a significant improvement of the elongation at break, yielding a much more ductile

and tougher material. In addition, the presence of PMMA-functionalized GO also stabilized the nanocomposites increasing the onset of thermal decomposition by around 50 °C.

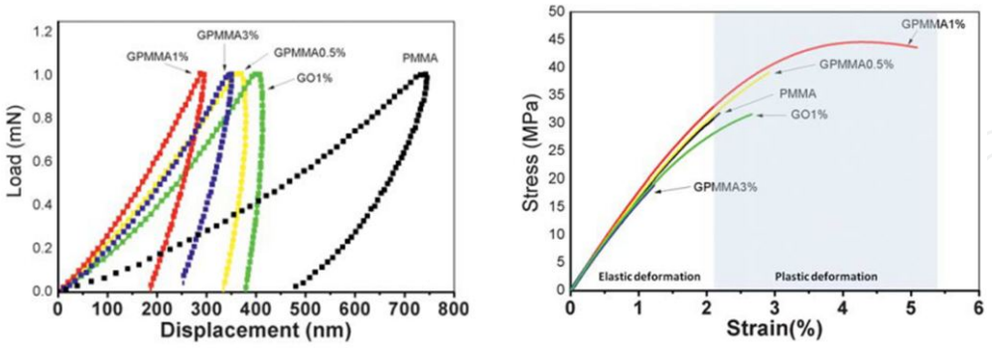

Figure 3. Load-displacement nanoidentation (left) and stress-strain curves (right) of films of PMMA and its nanocomposites with PMMA-functionalized graphene. [40]

Yang et al. [42] also took advantage of the carboxylic groups to graft poly-(2-dimethylaminoethyl methacrylate) (PDMAEMA) onto GO sheets. Here, the BMPB initiators were attached onto GO sheets by two steps involving amidation reactions. This functionalization of GO with PDMAEMA not only enhanced the solubility in acidic aqueous solutions (pH = 1), but also in short chain alcohols. Moreover, this solubility allowed this functionalized-GO to be mixed with spherical particles of poly(ethylene glycol dimethacrylate-co-methacrylic acid) to generate decorated GO sheets.

3.1.2. Other polymerization methods apart from ATRP

Besides the ATRP method, polycondensation, [33] ring opening polymerization [34], reversible addition-fragmentation chain transfer (RAFT) mediated mini-emulsion polymerization [35], direct electrophilic substitution [36], and Ziegler–Natta polymerization [37] have also been used to functionalize the graphene sheets with various polymer chains, which will be discussed below.

Wang et al. [33] functionalized GO sheets with polyurethane (PU) by using the polycondensation method. Here GO sheets were reacted with 4,4′-diphenylmethane diisocyanate followed by polycondensation of poly(tetramethylene glycol) and ethylene glycol. The presence of PU chains linked to GO remarkably improved the dispersion of GO in PU matrix, which was confirmed by the morphological study, and make it compatible with pure PU forming strong interfacial interactions that provide an enhanced load transfer between the matrix and the GO sheets thus improving their mechanical properties, as well as their thermal properties. With the incorporation of 2.0 wt% PU-functionalized GO, the tensile strength and storage modulus of the PU nanocomposites increased by 239% and 202%, respectively (Figure 4). Furthermore, the nanocomposites displayed high electrical conductivity, and improved thermal stability of PU was also achieved (Figure 4).

http://dx.doi.org/10.5772/50490

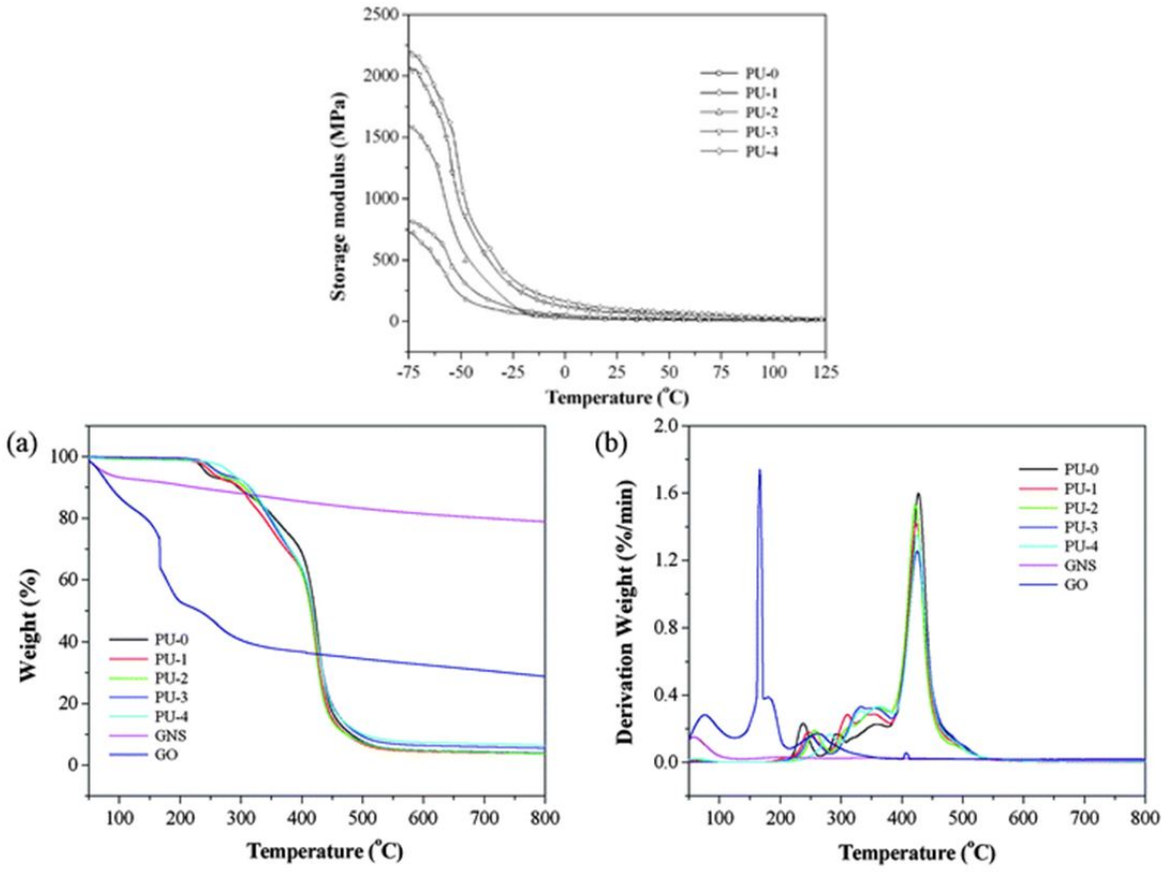

Figure 4. The improved thermal and mechanical propertied of PU/GO nanocomposites [33].

Etmimi et al. [35] investigated the preparation of PS/GO nanocomposites via RAFT mediated mini-emulsion polymerization. In this process, dodecyl isobutyric acid trithiocarbonate (DIBTC) RAFT agent was attached to the hydroxyl groups of GO through an esterification reaction (Figure 5). The resultant RAFT-grafted GO was used for the preparation of PS/GO nanocomposites in miniemulsion polymerization. The stable miniemulsions were obtained by sonicating RAFT-grafted GO in styrene monomer in the presence of a surfactant, followed by polymerizing using AIBN as the initiator to yield encapsulated PS-GO nanocomposites. The molecule weight and polydispersity of PS in the nanocomposites depended on the amount of RAFT-grafted GO in the system, in accordance with the features of the RAFT polymerization method. The thermal stability of the obtained PS/GO nanocomposites was improved, which may be attributed to the intercalation of PS into the lamellae of graphite. Furthermore, the increased RAFT-grafted GO significantly resulted in the improved mechanical properties of the nanocomposites. The storage and loss modulus of the nanocomposites were higher than those of the standard PS when the GO loadings reached 3 and 6%, respectively. Oppositely, as RAFT-grafted GO content increased, the T_g values of the sample decreased. This was attributed to the change in the molecule weight of the PS chains in the nanocomposites.

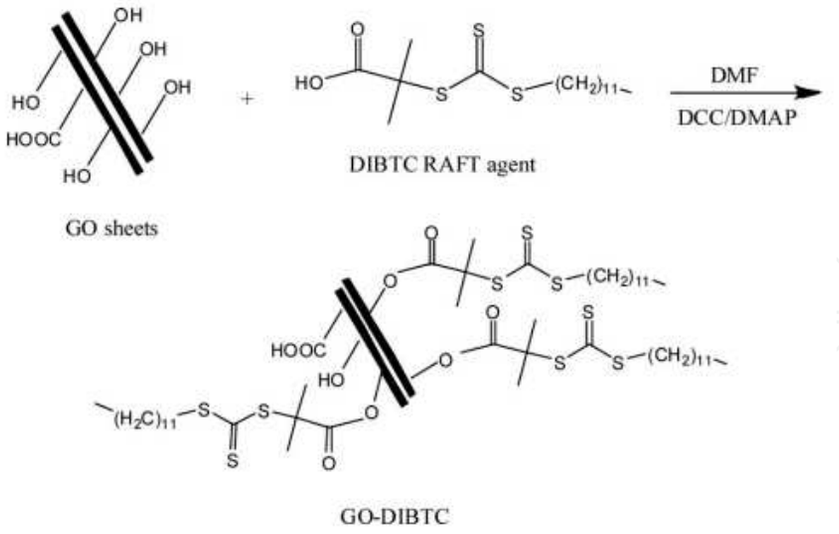

Figure 5. The overall synthesis route for the preparation of RAFT immobilized GO nanosheets [35].

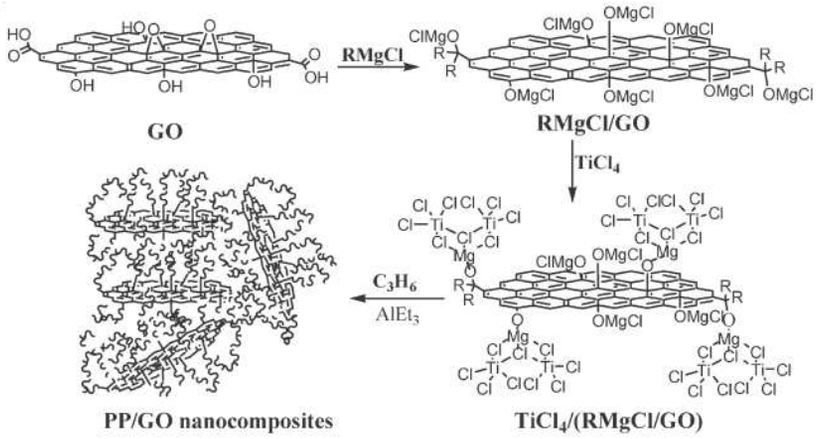

Figure 6. Fabrication of PP/GO nanocomposites by in situ Ziegler-Natta polymerization [37].

Huang et al. [37] reports the first example of preparation of polypropylene/GO (PP/GO) nanocomposites via in situ Ziegler−Natta polymerization. As illustrated in Figure 6, a Mg/Ti catalyst species was immobilized onto GO sheets by reacting with the surface functional groups including −OH and −COOH. Subsequent propylene polymerization led to the in situ formation of PP matrix, which was accompanied by the nanoscale exfoliation of GO. Independent of the opposing nature of the polymer and GO, a good dispersion of GO sheets in PP matrix was observed, which was verified by morphological examination through TEM and SEM observation. Furthermore, high electrical conductivity was discovered with thus prepared PP/GO nanocomposites, this being the only paper reporting conductive materials prepared by grafting a polymer from graphene sheets. For example, at a GO loading of 4.9

wt %, σ_c was measured at 0.3 S m^{-1}. We believe that this must originate from a side reaction involving the reduction of GO sheets that occurs in one of the synthetic steps.

3.1.3. Irradiation-induced polymerization

Ultrasound has found important applications in a diverse range of materials and chemical syntheses [48, 51]. Both the physical and chemical effects of ultrasound arise from acoustic cavitation: the formation, growth, and collapse of bubbles in liquids irradiated with high intensity ultrasound [48 - 50, 52]. Localized hot spots with temperature of ~5000K and pressures of hundreds of bars are generated during the bubble collapse within liquid, which can induce some chemical reactions that can't take place under normal conditions. Xu et al. [53] reported a convenient single-step sonication-induced approach for the preparation of polymer functionalized graphenes from graphite flakes and a reactive monomer, styrene. In this work, they showed that by choosing a reactive medium as the solvent, the combined mechanochemical effects of high intensity ultrasound can, in a single step, readily induce exfoliation of graphite to produce functionalized graphenes. Ultrasonic irradiation of graphite in styrene results in the mechanochemical exfoliation of graphite flakes to single-layer and few-layer graphene sheets combined with functionalization of the graphene with PS chains (Figure 7). The PS chains are formed from sonochemically initiated radical polymerization of styrene. They also tested a variety of other solvents, including toluene, ethylbenzene, 1-dodecene, and 4-vinylpyridine to prepare functionalized graphenes. Only the easily polymerizable reactants containing vinyl groups, styrene and 4-vinylpyridine, lead to stable functionalized graphene. Such functionalized graphene have good stability and solubility in common organic solvents and have great potential for graphene-based composite materials.

Moreover, direct photografting reactions of vinyl monomers came into focus for the preparation of stable polymer brushes. Two approaches in particular, the sequential "living" photopolymerization and the self-initiated photografting and photopolymerization (SIPGP), attracted the attention of numerous research groups because of the facile preparation and broad applicability. Steenackers et al. [54] showed that PS chains could covalently bound to graphene by the UV-induced polymerization of styrene (Figure 8). Photopolymerization occurs at existing defect sites and that there is no detectable disruption of the basal plane conjugation of graphene. This method thus offers a route to define graphene functionality without degrading its electronic properties. Furthermore, photopolymerization with styrene results in self-organized intercalative growth and exfoliation of few layer graphene sheets. Under these reaction conditions, a range of other vinyl monomers exhibits no reactivity with graphene. However, the authors demonstrate an alternative route by which the surface reactivity can be precisely tuned, and these monomers can be locally grafted via electron-beam-induced carbon deposition on the graphene surface.

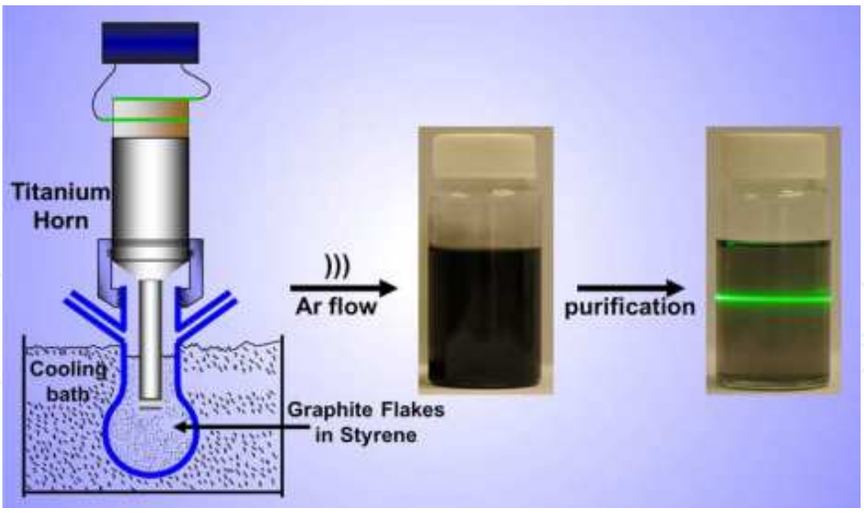

Figure 7. Experimental setup of the one-step mechanochemical process for exfoliation of graphite and sonochemical functionalization of graphene [53].

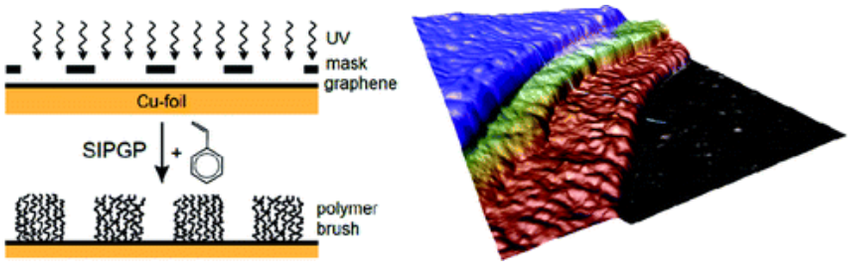

Figure 8. Patterned polymer brush layers on CVD-grown single layer graphene are prepared by UV illumination through a mask in bulk styrene. Surface photopolymerization occurs selectively in illuminated regions of the material [54].

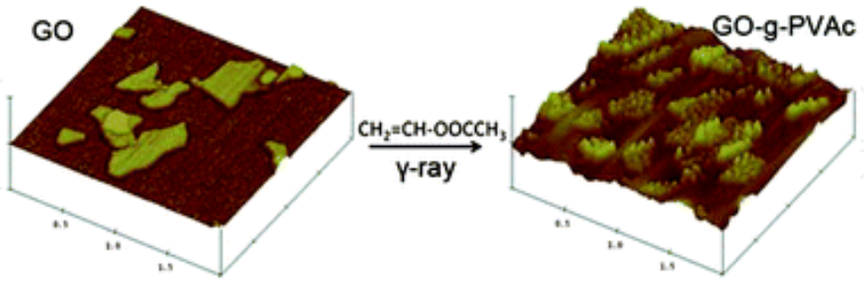

Figure 9. The preparation of PVAc grafted GO by γ-ray irradiation-induced graft polymerization [55].

γ-ray radiation-induced graft polymerization has many advantages, including being a single-step chemical reaction, needing no additives or catalysts, being conducted at room temperature, cost-effective, and so on. Above all, it is versatile for vinyl monomers that undergo free radiation polymerization, and production can be easily scaled-up. Zhang et al. [55] reported a facile approach to functionalize GO sheets with poly(vinyl acetate) (PVAc) by

γ-ray irradiation-induced graft polymerization (Figure 9). Due to the full coverage of PVAc chains and solvated layer formation on GO sheets surface, which weakens the interlaminar attraction of GO sheets, PVAc-functionalized GO was well dispersed in common organic solvents, and the dispersions obtained were extremely stable at room temperature without any aggregation.

Furthermore, Lee at al. [56] have developed a method to selectively fluorinate graphene by irradiating fluoropolymer-covered graphene with a laser (Figure 10). Here the sp^2-hybrized graphene would react with the active fluorine radicals, which was produced by photon-induced decomposition of the fluoropolymer under laser-irradiation, and form C-F bonds. However, this reaction only occurred in the laser-irradiated region. The kinetics of C–F bond formation is dependent on both the laser power and fluoropolymer thickness. Furthermore, the resistance of the graphene dramatically increased due to the fluorination, while the basic skeletal structure of the carbon bonding network is maintained. This is an efficient method for isolating graphene devices because the laser irradiation on fluoropolymer-covered graphene process produces fluorinated graphene with highly insulating properties in a single step.

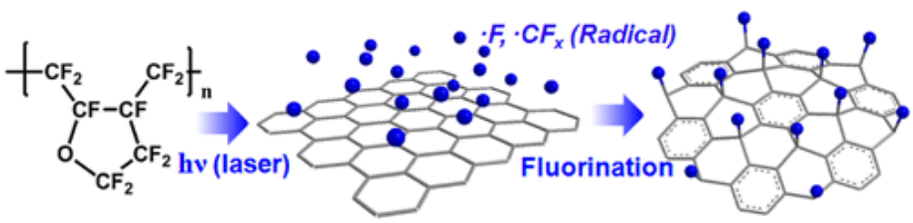

Figure 10. The scheme showing a mechanism for fluorination under laser-irradiation.[56]

3.2. Functionalizations via "grafting to" method

As commented previously, the "grafting from" method relies on the immobilization of initiators at the surface of graphene, followed by in situ surface-initiated polymerization to generate tethered polymer chains. However, this may not be possible in certain cases, where the covalent linkage between the presynthesized polymer and graphene emerges as the only alternative. In order to expand the type of polymers that can be bound to graphene, the category of "grafting-to" method can be employed to achieve this purpose. The "grafting to" technique involves the bonding of preformed end functionalized polymer chains to the surface of graphene. Therefore, the prepared graphene require adequate functional groups, which could react with specific polymers. Or the polymer has functionalities capable of reacting with either graphene or its chemically broader cousin, GO. In the following part, we will summarize the type of reactions and the families of polymers that have been grafted to the graphene.

3.2.1. Esterification/amidation reactions

Esterification/amidation reactions between carboxylic groups in GO and hydroxyl or amine groups in the polymer have been widely investigated [14, 15, 44, 57, 60]. In this respect, poly(vinyl alcohol) (PVA) was covalently bonded to GO [14, 57] and r-GO [14] by using a typical catalytic system for esterification (Figure 11). After functionalization with PVA chains, the solution processability of graphene was significantly improved. And the degree of functionalization was shown to be low, probably due to steric hindrance caused by the huge volume of GO. However, due to the presence of the huge graphene sheets, significant changes in the crystalline properties as well as in the tacticity of the polymer were observed. The originally semicrystalline PVA became completely amorphous, and the T_g increased by 35 °C after bonded to GO sheets. The decrease in crystallinity was attributed to the intercalation of PVA chains between the graphene sheets as well as the formation of "secondary" bonds, for example, hydrogen bonding that breaks intra- and interchain bonds. Finally, it has been demonstrated that the reaction is favoured at specific conformations at the isotactic sequences where the hydroxyl groups are more exposed (lower internal steric hindrance) than in the syndiotactic counterpart.

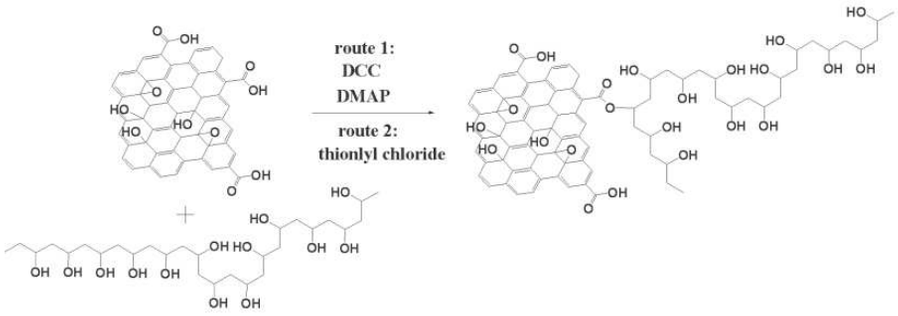

Figure 11. Schematic Illustration of the Esterification of GO with PVA [14].

A similar strategy has been approached to functionalize r-GO with poly(vinyl chloride) (PVC) [59]. In this step, the susceptible groups in PVC chains could react with the functional groups on r-GO sheets by esterification, which was provided by a nucleophilic substitution reaction [61, 62]. Furthermore, several methodologies to prepare r-GO/PVC nanocomposites and the optimum conditions have been established. The covalent attachment of r-GO to appropriately functionalized PVC is the only effective method to produce nanocomposites with improved thermal and mechanical properties (Figure 12). The absolute values of the mechanical and thermal properties of PVC-functionalized GO nanocomposites are higher than those for a similar system using MWNTs as reinforcement because of the higher aspect ratio of the r-GO sheets with respect to the MWNTs. The introduction of r-GO also increases the T_g of the composites, reflecting the changes in the mobility of the PVC chains. However, due to the lower strength of the "secondary bonds", such as halogen bonding and hydrogen bonding for PVC and PVA respectively, the changes in T_g for PVC were much lower than those reported for PVA, which had a similar degree of functionalization with PVC-function-

http://dx.doi.org/10.5772/50490

alized GO. The existence of these secondary bonds can lead to some additional ordering that alters the segmental mobility and consequently the final properties.

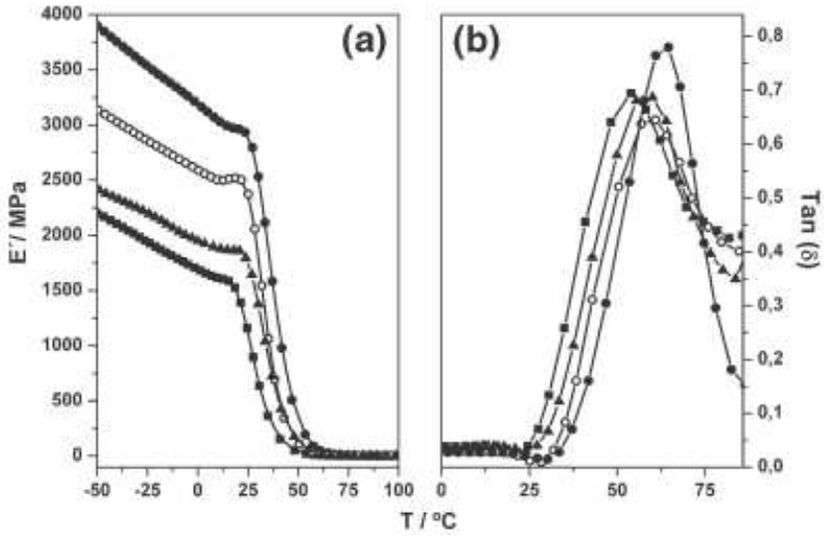

Figure 12. Comparison of (a) storage modulus and (b) tan δ curves for neat PVC (square), PVC functionalized CNTs (triangle), PVC functionalized GO (solid circle), and PVC functionalized r-GO (open circle) [59].

Furthermore, conjugated polymer-functionalized graphene materials have also been prepared by esterification/amidation reactions [60, 63]. In these cases, the ends of the conjugated polymers were bonded to the functional groups on the graphene sheets. As a result, the solubility of the obtained functionalized graphene was significantly improved in common solvents, enabling device preparation by solution processing. Thus, GO functionalized with both triphenylamine-based polyazomethine-modified GO (TPAPAM-GO) and poly(3-hexylthiophene) modified GO (P3HT-GO) (Figure 13) can be incorporated into specific devices by simple spin coating to obtain composites that exhibit non-volatile memory effect as well as higher power conversion efficiency for solar cells, demonstrated in the cases of TPAPAM-GO and P3HT-GO, respectively.

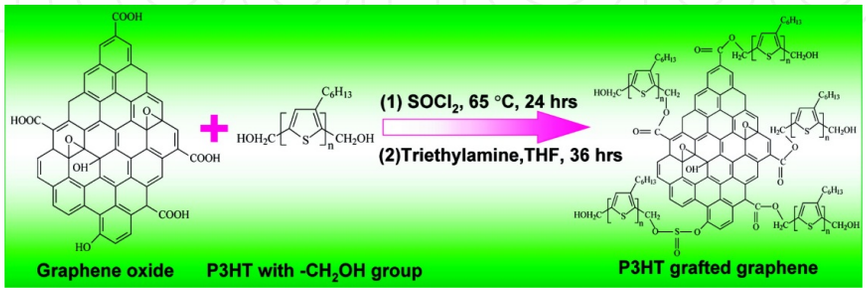

Figure 13. Synthesis procedure for chemical grafting of CH_2OH-terminated P3HT chains onto graphene, which involves the $SOCl_2$ treatment of GO (step 1) and the esterification reaction between acyl-chloride functionalized GO and MeOH-terminated P3HT (step 2) [47].

3.2.2. Nitrene cycloaddition

Nitrene chemistry, an approach used to functionalize graphene with single molecules [64, 65], has also been extended to polymers [66, 67].Nitrene chemistry is a versatile tool that allows the functionalization of graphene with a pool of functionalities, potentiating graphene solubility, and dispersion in a wide variety polymeric matrices. By using of this technology, He and Gao [67] have reported a general and versatile approach to graft of polymers onto graphene sheets. In their experiment, a wide range of immobilized functional groups were used to graft specific polymers from it (Figure 14). Though the cycloadditions of nitrene radicals and thermal reduction of GO occurs simultaneously, the conductivity of graphene diminished after functionalization, values of around 300-700 S/m for PS and poly(ethylene glycol) (PEG)-functioanlzied graphene were obtained. This was mainly due to the high amounts of graphene in the final product, which is reasonable because although the polymer is linked to graphene by the ends, the molecular weight of the polymers is low, making the mass percentage of graphene high.

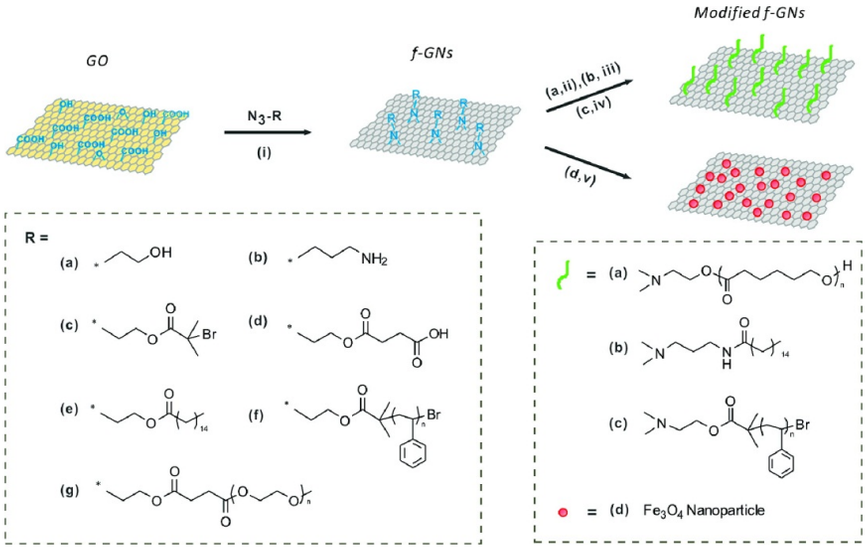

Figure 14. General strategy for the preparation of functionalized graphene sheets by nitrene chemistry and the further chemical modifications [67].

Besides the methods mentioned above, other "grafting to" approaches have also been investigated, such as the opening of maleic rings in maleic acid (MA) grafted polyethylene by amine functionalized graphene [68], nucleophilic epoxy-ring opening in GO by amine groups in biocompatible poly-l-lysine [69], atom transfer nitroxide radical coupling (ATNRP) of PNIPAM and 2,2,6,6-tetramethylpiperidine-1-oxyl-modified graphene [70], and simultaneous reduction of GO and radical grafting of PMMA by phase transfer [71].

3.2.3. Irradiation-induced radical grafting

Shen et al. [72] have reported PVA-functionalized graphene (f-G) could be prepared by ultrasonication of pristine graphene (p-G) in a PVA aqueous solution (Figure 15). Ultrasonic

http://dx.doi.org/10.5772/50490

irradiation of graphene can cause a considerable amount of defects on the graphene surface, which might produce reactive sites in situ as a result of the high temperature and pressure during bubble collapse. Moreover, the original defects on pristine graphene can also be easily destroyed and produce reactive sites during ultrasonic irradiation. The PVA chain radicals produced by sonochemical degradation of the PVA solution can react easily with graphene, because of the reactive sites formed on the graphene surface, and readily functionalized them via "grafting to" method. The content of PVA on graphene was estimated to be ~35%. The f-G could be well dispersed in the PVA matrix by a simple solution mixing and casting procedure. Due to the effective load transfer between f-G and PVA matrix, the mechanical properties of the f-G/PVA films were significantly improved. Compared with the p-G/PVA films, a 12.6% increase in tensile strength and a 15.6% improvement of Young's modulus were achieved by addition of only 0.3 wt% f-G. Moreover, this simple ultrasonication technique could enable us to functionalize graphene with other polymers.

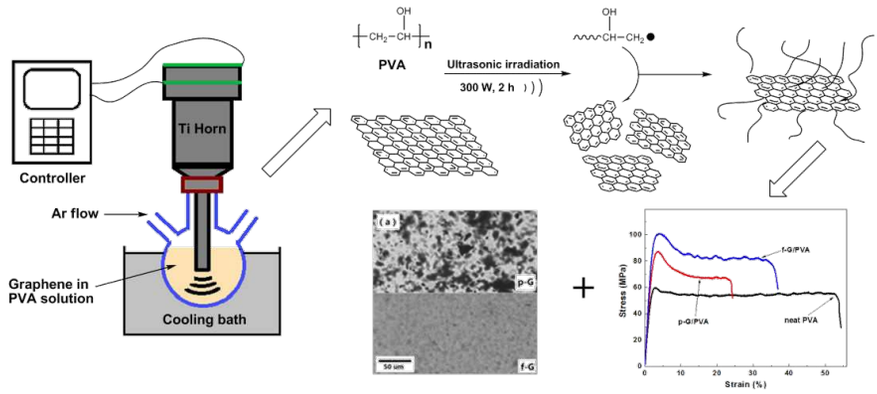

Figure 15. Schematic illustration of the sonochemical preparation process of PVA-functionalized graphene [72].

As a summary, "grafting-to" methods are highly versatile since they take advantage of the chemistry of GO that can be appropriately modified with a wide variety of functional groups providing a capacity for reaction with almost any type of polymers. In addition, "grafting-to" method allows the selection of the location of graphene, that is, at the end or as part of the main chain that can be directly related to changes in the final properties.

4. Non-covalent functionalization of graphene with polymers

As shown in the aforementioned examples, the covalent functionalization of polymers on graphene-based sheets holds versatile possibility due to the rich surface chemistry of GO/r-GO. Nevertheless, the non-covalent functionalization, which almost relies on hydrogen bonding or π–π stacking, is easier to carry out without altering the chemical structure of the capped r-GO sheets, and provides effective means to tailor the electronic/optical property and solubility of the nanosheets. The first example of non-covalent functionalization of r-GO sheets was demonstrated by the in situ reduction of GO with hydrazine in the presence of

poly(sodium 4-styrenesulfonate) (PSS) [12], in which the hydrophobic backbone of PSS stabilizes the r-GO, and the hydrophilic sulfonate side groups maintains a good dispersion of the hybrid nanosheets in water.

4.1. Functionalizations via π–π stacking interactions

π–π stacking interactions usually occur between two relatively large non-polar aromatic rings having overlapping π orbitals. They can be comparable to covalent attachment in strength and hence provide more stable alternatives to the weaker hydrogen bonding, electrostatic bonding and coordination bonding strategies. Furthermore, π–π stacking functionalization does not disrupt the conjugation of the graphene sheets, and hence preserves the electronic properties of graphene.

4.1.1. Polymers with pyrene end-groups

In order to functionalize graphene with polymers via π–π stacking, one strategy is for the polymer chains to be synthesized with pyrene moieties as the termini of the polymer chains. RAFT polymerization can be a useful tool to achieve this aim. Polymers with pyrene end-groups have been made using RAFT mechanism in several recent papers [73, 80].

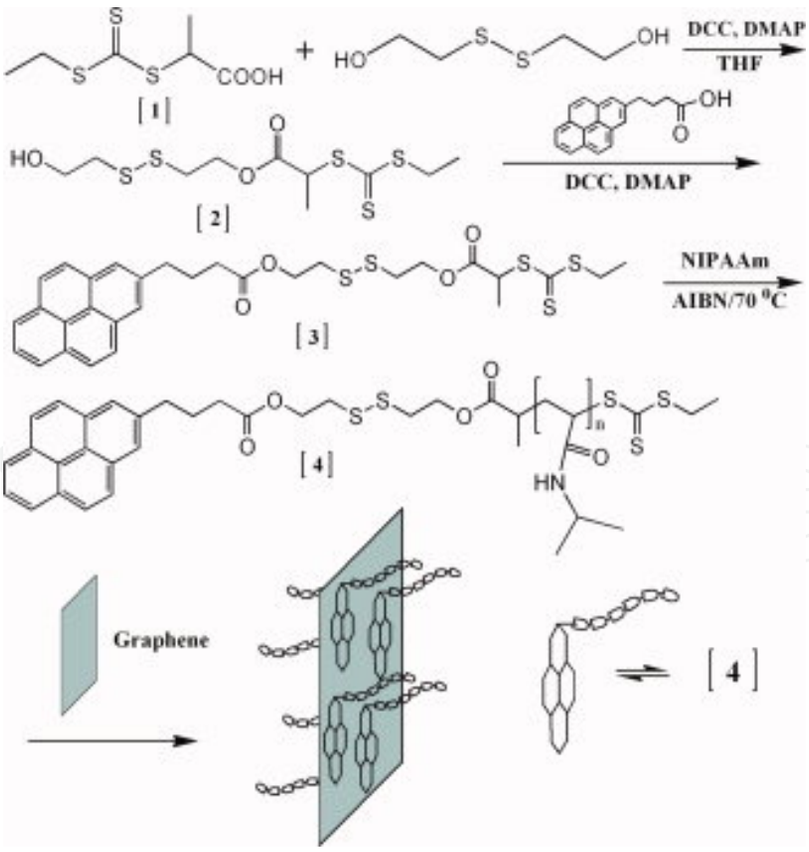

Figure 16. A schematic depicting the synthesis of pyrene-terminated PNIPAAm using a pyrene-functional RAFT agent and the subsequent attachment of the polymer to graphene [81].

http://dx.doi.org/10.5772/50490

Liu et al. synthesized thermoresponsive graphene-polymer nanocomposites. They first took advantage of RAFT polymerization to synthesize a well-defined thermoresponsive pyrene terminated poly(N-isopropylacrylamide) (PNIPAAm), followed by attachment onto the basal plane of graphene sheets via π-π stacking interactions (Figure 16) [81]. The lower critical solution temperature (LCST) of pyrene-terminated PNIPAAm was measured to be 33 ° C. However, after the pyrene-functional polymer functionalized with graphene sheets, the resultant graphene composites were also thermoresponsive in aqueous solutions, but with a lower LCST of 24 °C.

Similarly, Liu et al. also prepared pH sensitive graphene-polymer composites by functionalization of graphene with a pyrene-terminated positive charged polymer, poly(2-N,N′-(dimethyl amino ethyl acrylate)) (PDMAEA), and a negatively charged polymer, polyacrylic acid (PAA) [80]. During the process, a pyrene-terminated RAFT agent was used to prepare the pyrene-terminated PDMAEA and PAA. When manipulating the pH of the graphene –composite suspensions, phase transfer between the aqueous and organic phases was observed. Self-assembly of the two oppositely charged graphene-polymer composites afforded layer-by-layer (LbL) structures as evidenced by high-resolution scanning electron microscopy (SEM) and quartz crystal microbalance (QCM) measurements (Figure 17). In addition to RAFT mechanism, π-orbital rich polymers have also been synthesized by using of ATRP method for functionalization of r-GO to afford the fluorescent and water-soluble graphene composites via π-π stacking interactions [82].

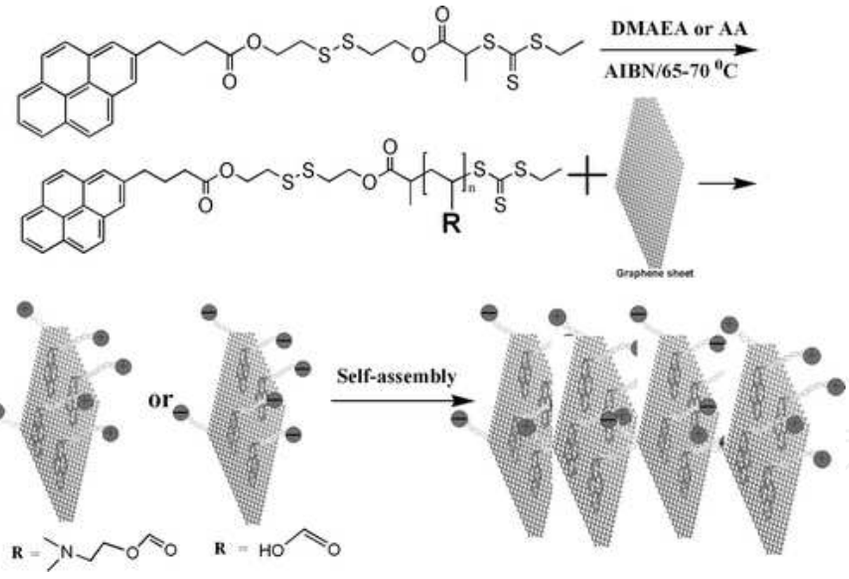

Figure 17. Synthesis of pH sensitive pyrene-polymer composites via π-π stacking interactions for the self-assembly of functionalized graphene into layered structures [80].

4.1.2. Conjugated polyelectrolytes

Moreover, conjugated polyelectrolytes with various functionalities have been used to modify r-GO nanosheets [83 - 85], in the hope to achieve good solubility in different kinds of sol-

vents, and at the same time acquire added optoelectronic properties. Qi et al. has specially designed an amphiphilic coil–rod–coil conjugated triblock copolymer (PEG-OPE, chemical structure shown in Figure 18A) to improve the solubility of graphene-polymer nanocomposites in both high and low polar solvents [33, 83]. In the proposed configuration, the conjugated rigid-rod backbone of PEG-OPE can bind to the basal plane of the r-GO via the π-π stacking interaction (Figure 18B), whereas the lipophilic side chains and two hydrophilic coils of the backbone form an amphiphilic outer-layer surrounding the r-GO sheet. As a result, the obtained r-GO sheets with a uniformly coated polymer layer (Figure 18C) are soluble in both organic low polar (such as toluene and chloroform) and water-miscible high polar solvents (such as water and ethanol).

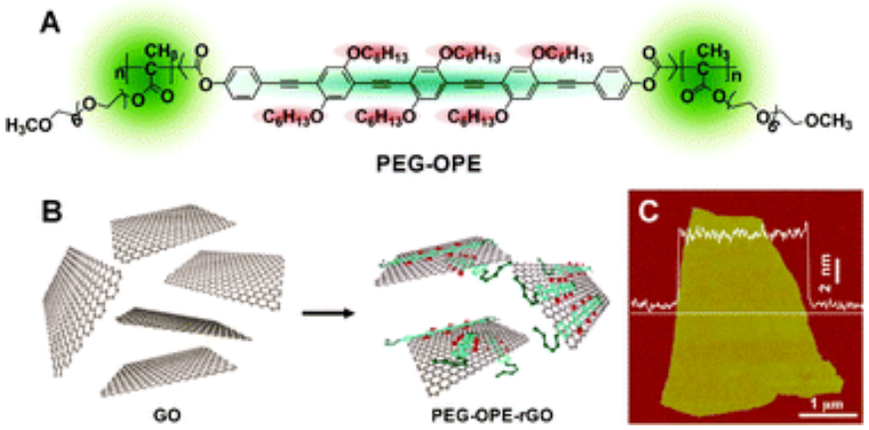

Figure 18. A) Chemical structure of PEG-OPE. (B) Schematic illustration of fabrication of PEG-OPE stabilized r-GO sheets. (C) Tapping-mode AFM image and cross-sectional analysis of PEG-OPE-r-GO on mica [67].

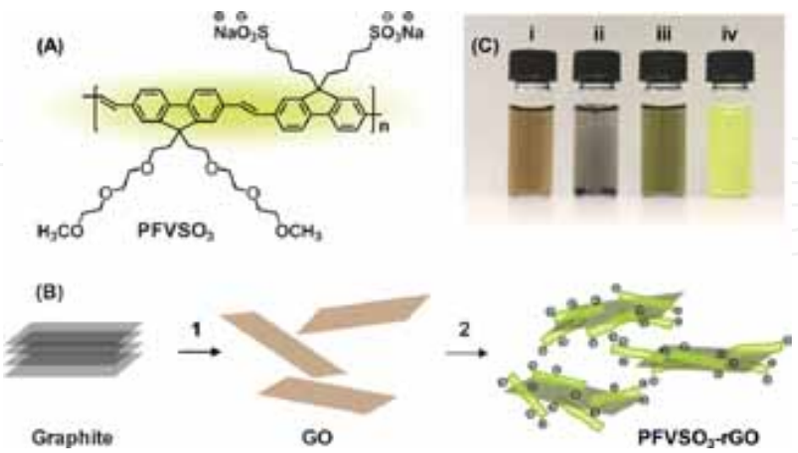

Figure 19. A) Chemical structure of the newly designed $PFVSO_3$. B) Schematic illustration of the synthesis of $PFVSO_3$-stabilized r-GO in H_2O: step 1, oxidative treatment of graphite (gray-black) yields single-layer GO sheets (brown); step 2, chemical reduction of GO with hydrazine in the presence of $PFVSO_3$ produces a stable aqueous suspension of $PFVSO_3$-functionalized r-GO sheets ($PFVSO_3$-r-GO). C) Photograph of aqueous dispersions of GO (i), r-GO (ii), $PFVSO_3$-r-GO (iii), and $PFVSO_3$ (iv) [84].

In another study, Qi et al. demonstrated the preparation of highly soluble r-GO hybrid material ($PFVSO_3$-r-GO) by taking advantage of strong π–π interactions between the anionic CPE and r-GO (Figure 19) [84]. The resulting CPE-functionalized r-GO (PFVSO3-r-GO) shows excellent solubility and stability in a variety of polar solvents, including water, ethanol, methanol, dimethyl sulfoxide, and dimethyl formamide. The morphology of $PFVSO_3$-r-GO is studied, which reveal a sandwich-like nanostructure. Within this nanostructure, the backbones of $PFVSO_3$ stack onto the basal plane of r-GO sheets via strong π–π interactions, while the charged hydrophilic side chains of $PFVSO_3$ prevent the rGO sheets from aggregating via electrostatic and steric repulsions, thus leading to the solubility and stability of $PFVSO_3$-rGO in polar solvents. Furthermore, the presence of $PFVSO_3$ within r-GO induces photoinduced charge transfer and p-doping of r-GO. As a result, the electrical conductivity of $PFVSO_3$-r-GO is not only much better than that of GO, but also than that of the unfunctionalized r-GO.

4.1.3. π–π stacking induced by melt blending

High temperature and strong shear forces are usually involved during the melt blending process, which tends to fracture the nanoparticle aggregates, and endow polymer chains with the ability to diffuse into the gaps of the nanoparticle interlayer. Furthermore, as suggested by theoretical and experimental studies [86, 87] chemical or physical interactions can be formed between the fillers and the polymer components. Zhang et al [88] found the melt blending led to enhanced interactions between PS and CNTs, which was indicated by increased amount of PS linked to CNTs and therefore dramatically increased solubility of CNTs in some solvents. Taking advantage of this method, Zhou et al [89] obtained PS-coated CNTs through simple melt mixing of PS with CNTs. Furthermore, Lu et al [90] studied the styrene-butadiene-styrene tri-block copolymer (SBS)/CNTs composite, and their results showed that there were interactions between CNTs and SBS occurred during melt mixing, leading to an improvement of the mechanical properties of SBS/CNTs composites, as well as the homogeneous dispersion of CNTs in SBS. The mechanism of melt blending on these enhanced interactions was mainly attributed to the formation of π-π stacking between the aromatic system of π-electrons of PS and the π-electrons system of CNTs during melt blending [10, 88].

Melt Blending can also graft PS chains onto the surface of graphene sheets via π-π interactions. The interaction between graphene and PS was significantly enhanced by melt blending, which led to an increased amount of PS-functional graphene (PSFG) exhibiting good solubility in some solvents [10]. The mechanism for the in-situ formation of π-π stacking was addressed, as illustrated in Figure 20. It was proposed that the strong shear action applied by extruder could stretch the PS chains and endow the polymer chains with possibility to diffuse into the interlayer gap of graphene sheets. Moreover, the PS chains could be pushed towards to graphene sheets to form the π-π stacking under high shear forces. The UV-vis absorption spectroscopy of PSFG presented an obvious red shift, suggested the presence of π-π stacking between PS and graphene.

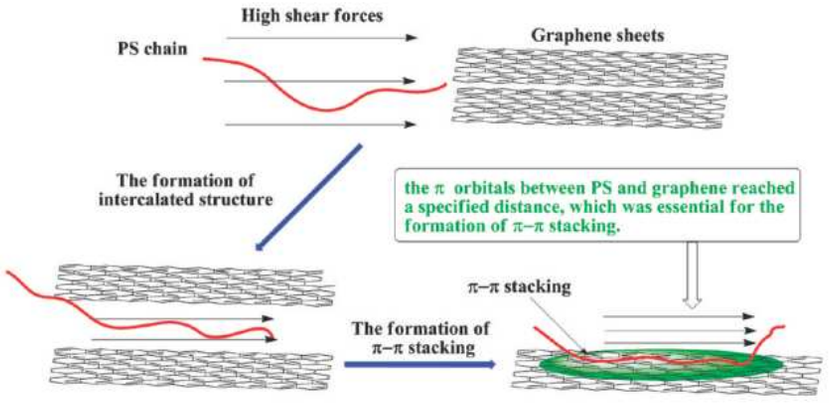

Figure 20. Schematic for the forming of π-π stacking in the process of melt blending [10].

4.2. Functionalizations via hydrogen bonding

Hydrogen bonding is very common in the biological world. An individual hydrogen bond is not very strong (2–8 kcal/mol); however, multiple hydrogen bonds will afford strong interactions as seen in DNA hybridization. Liang et al. prepared PVA nanocomposites with graphene by dispersing GO sheets into PVA matrix at molecular level [91]. The authors considered that the increased tensile strength and Young's modulus of the PVA/GO composite films were caused by the strong hydrogen bonding interactions between the residual oxygen-containing groups of GO sheets, such as epoxides and hydroxyls on their basal planes and carboxyls on the edges, and hydroxyl groups of the PVA chains. Polymer/graphene nanocomposites with other hydrophilic polymers, epoxy, poly(acrylonitrile) and polyaniline exhibited extraordinary high increase in modulus or glass transition temperature, attributed to hydrogen bonding interactions [92 - 94].

5. Applications of functionalized graphene

The use of graphene or functionalized graphene materials usually exploits properties such as the large surface area or high electrical conductivity. Currently, the applications of functionalized graphene are focused on clean energy devices and electronic devices, as well as on sensors, medical devices and catalysis. Two examples will be discussed below.

Non-covalent chemical modification between functionalized pyrene and graphene was adopted to achieve patterned arrays of glucose oxidase (GOD) for potential applications in glucose sensors, cell sensors and tissue engineering [96]. In research by Zeng et al. as illustrated in Figure 21, [95] chemically reduced GO was functionalized by pyrene-grafted poly(acrylic acid) (PAA) in aqueous solution on the basis of π-π stacking as well as van der Waals interactions. Then PAA-functionalized graphene (PAA-graphene) was LbL assembled with poly(ethyleneimine) (PEI). Graphene multilayer films facilitated the electron transfer, enhancing the electrochemical reactivity of H_2O_2. On the basis of this property, they

http://dx.doi.org/10.5772/50490

fabricated a bienzyme biosensing system for the detection of maltose by successive LbL assembly of functionalized graphene, GOD, and glucoamylase (GA), which showed great promise in highly efficient sensors and advanced biosensing systems.

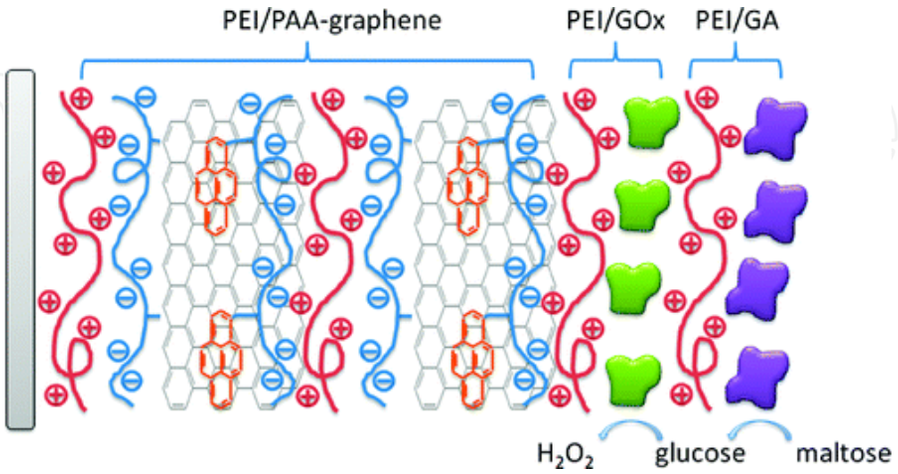

Figure 21. Schematic Illustration of the Strategies for layer-by-layer assembly of graphene multilayer films for enzyme-based glucose and maltose biosensing [95].

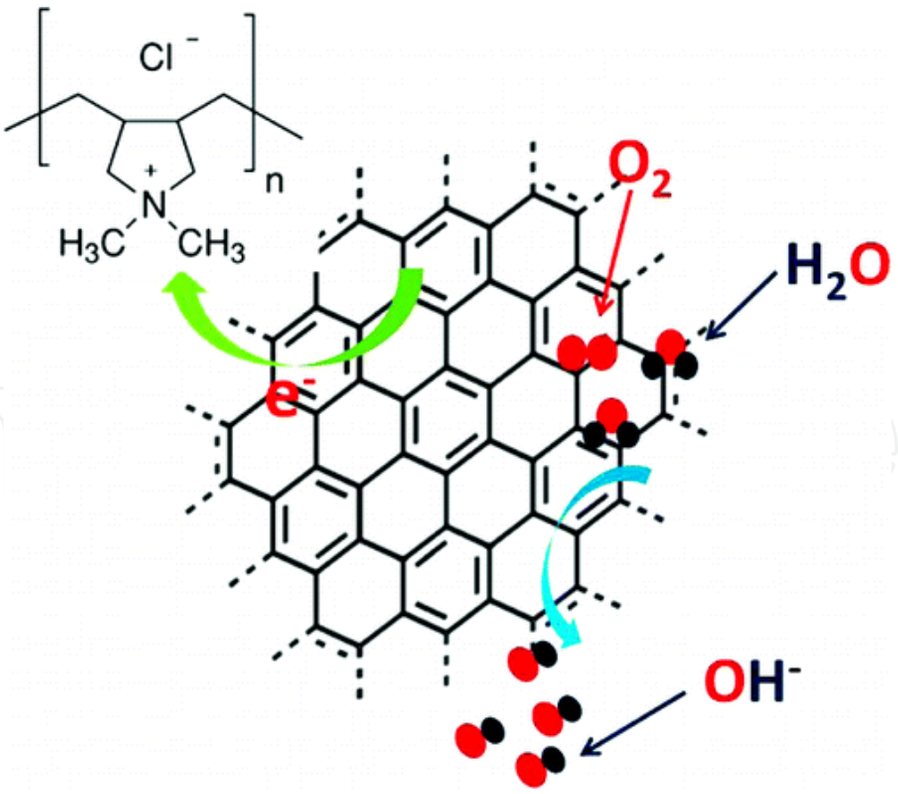

Figure 22. Schematic illustration of the electron-withdrawing from graphene by PDDA to facilitate the ORR process [97].

The planar structure and superb conductivity of graphene also provide an appropriate platform for novel electrochemical sensors. A metal-free electrocatalyst for the oxygen reduction reaction (ORR) was achieved with graphene sheets functionalized with an electron acceptor, poly(diallyldimethylammonium chloride) (PDDA) (Figure 22). The resultant positively charged graphene composite was demonstrated to show remarkable electrocatalytic activity toward ORR with better fuel selectivity, tolerance to CO poisoning, and long-term stability than that of the commercially available Pt/C electrode [97]. The observed ORR electrocatalytic activity induced by the intermolecular charge-transfer provides a general approach to various carbon-based metal-free ORR catalysts for oxygen reduction.

6. Conclusion

Generally speaking, functionalization of graphene with polymers can be achieved via either covalent or non-covalent interactions. Furthermore, the functionalization of graphene is always based on the graphene from previously prepared GO, which has multiple oxygen-containing functionalities, such as hydroxyl and carboxyl groups. In the covalent functionalizations, "grafting to" and "grafting from" techniques have been developed to graft the polymer chains onto the graphene surface. The "grafting from" method relies on the immobilization of initiators at the surface of graphene, followed by in situ surface-initiated polymerization to generate tethered polymer chains. The "grafting to" technique involves the bonding of preformed end functionalized polymer chains to the surface of graphene. Comparing both methods through the examples described above, it seems that "grafting-to" method allows the covalent bonding of a wider variety of polymers to graphene. The polymers "grafted from" graphene are those produced principally by some type of radical polymerization, such as ATRP and RAFT. However, the most relevant polymers grafted from graphene, such as PS and PMMA have also been attached to graphene by the "grafting-to" method. In principle, for polymers obtained by ATRP the "grafting-from" method might be the most appropriate, but this depends on the features desired in the final composite, because through "grafting to" method graphene forms part of the bulk polymer whereas in the "grafting from" it is limited to a terminal group. Moreover, except for a few exceptions, functional polymers and polymers synthesized by condensation reactions are principally bound to graphene by the grafting-to approach. Regarding to use PVA and PVC to functionalize graphene, we select the "grafting to" method due to the experimental procedures employed to obtain these polymers. In fact, it is well known that PVA is not prepared by polymerization of the corresponding monomer, and the majority of PVC is synthesized by free-radical polymerization through suspension or bulk processes. Finally, radiation-induced graft polymerization has been utilized in the "grafting to" and "grafting from" techniques, due to its advantages, including being a single-step chemical reaction, needing no additives or catalysts, being conducted at room temperature, cost-effective, and so on.

The covalent functionalization of polymers on graphene-based sheets holds versatile possibility due to the rich surface chemistry of GO/r-GO. Nevertheless, the non-covalent functionalization, which almost relies on hydrogen bonding or π-π stacking, is easier to carry

out without altering the chemical structure of the capped rGO sheets, and provides effective means to tailor the electronic/optical property and solubility of the nanosheets. π-π stacking interactions usually occur between two relatively large non-polar aromatic rings having overlapping π orbitals. In order to functionalize graphene with polymers via π-π stacking, one strategy is for the polymer chains to be synthesized with pyrene moieties as the termini of the polymer chains. Moreover, conjugated polyelectrolytes with various functionalities have been used to functionalize graphene via π-π stacking. The hydrogen bonding interactions between the residual oxygen-containing groups of graphene sheets and hydroxyl groups of the hydrophilic polymer chains, such as PVA chains, have also been used to functionalize the graphene in order to obtain increased tensile strength and Young's modulus.

Author details

Wenge Zheng*, Bin Shen and Wentao Zhai

*Address all correspondence to: wgzheng@nimte.ac.cn

Ningbo Key Lab of Polymer Materials, Ningbo Institute of Material Technology and Engineering, Chinese Academy of Sciences, China

References

[1] Novoselov, K. S., Geim, A. K., Morozov, S. V., Jiang, D., Zhang, Y., Dubonos, S. V., Grigorieva, I. V., & Firsov, A. A. (2004). *Science*, 306, 666-669.

[2] Balandin, A. A., Ghosh, S., Bao, W., Calizo, I., Teweldebrhan, D., Miao, F., & Lau, C. N. (2008). *Nano Letters*, 8, 902-907.

[3] Lee, C., Wei, X., Kysar, J. W., & Hone, J. (2008). *Science*, 321, 385-388.

[4] Zhang, Y. W., Tan, W., Stormer, H. L., & Kim, P. (2005). *Nature*, 438, 201-204.

[5] Zhu, Y., Stoller, M. D., Cai, W., Velamakanni, A., Piner, R. D., Chen, D., & Ruoff, R. S. (2010). *ACS Nano*, 4, 1227-1233.

[6] Patil, A. J., Vickery, J. L., Scott, T. B., & Mann, S. (2009). *Advanced Materials*, 21, 3159-3164.

[7] Sudibya, H. G., He, Q., Zhang, H., & Chen, P. (2011). *ACS Nano*, 5, 1990-1994.

[8] Kuilla, T., Bhadra, S., Yao, D., Kim, N. H., Bose, S., & Lee, J. H. (2010). *Progress in Polymer Science*, 35, 1350-1375.

[9] Bai, H., Li, C., & Shi, G. (2011). *Advanced Materials*, 23, 1089-1115.

[10] Shen, B., Zhai, W., Chen, C., Lu, D., Wang, J., & Zheng, W. (2011). *ACS Applied Materials & Interfaces*, 3, 3103-3109.

[11] Bjo◉rk, J., Hanke, F., Palma, C. A., Samori, P., Cecchini, M., & Persson, M. (2010). *The Journal of Physical Chemistry Letters*, 1, 3407-3412.

[12] Stankovich, S., Piner, R. D., Chen, X., Wu, N., Nguyen, S. T., & Ruoff, R. S. (2006). *Journal of Materials Chemistry*, 16, 155-158.

[13] Huang, X., Qi, X., Boey, F., & Zhang, H. (2012). *Chemical Society Reviews*, 41, 666-686.

[14] Salavagione, H. J., Gómez, M. n. A., & Martínez, G. (2009). *Macromolecules*, 42, 6331-6334.

[15] Liu, Z., Robinson, J. T., Sun, X., & Dai, H. (2008). *Journal of the American Chemical Society*, 130, 10876-10877.

[16] Park, S., & Ruoff, R. S. (2009). *Nat Nano*, 4, 217-224.

[17] Staudenmaier, L. (1898). *Berichte der deutschen chemischen Gesellschaft*, 31, 1481-1487.

[18] Hummers, W. S., & Offeman, R. E. (1958). *Journal of the American Chemical Society*, 1958(80), 1339.

[19] Dreyer, D. R., Park, S., Bielawski, C. W., & Ruoff, R. S. (2010). *Chemical Society Reviews*, 39.

[20] Zhu, Y., Murali, S., Cai, W., Li, X., Suk, J. W., Potts, J. R., & Ruoff, R. S. (2010). *Advanced Materials*, 22, 3906-3924.

[21] Park, S., An, J., Jung, I., Piner, R. D., An, S. J., Li, X., Velamakanni, A., & Ruoff, R. S. (2009). *Nano Letters*, 9, 1593-1597.

[22] Stankovich, S., Dikin, D. A., Piner, R. D., Kohlhaas, K. A., Kleinhammes, A., Jia, Y., Wu, Y., Nguyen, S. T., & Ruoff, R. S. (2007). *Carbon*, 45, 1558-1565.

[23] Lomeda, J. R., Doyle, C. D., Kosynkin, D. V., , W., Hwang, F., & Tour, J. M. (2008). *Journal of the American Chemical Society*, 130, 16201-16206.

[24] Wang, H., Robinson, J. T., Li, X., & Dai, H. (2009). *Journal of the American Chemical Society*, 131, 9910-9911.

[25] Stankovich, S., Dikin, D. A., Dommett, G. H. B., Kohlhaas, K. M., Zimney, E. J., Stach, E. A., Piner, R. D., Nguyen, S. T., & Ruoff, R. S. (2006). *Nature*, 442, 282-286.

[26] Si, Y., & Samulski, E. T. (2008). *Nano Letters*, 8, 1679-1682.

[27] Wang, G., Yang, J., Park, J., Gou, X., Wang, B., Liu, H., & Yao, J. (2008). *The Journal of Physical Chemistry C*, 112, 8192-8195.

[28] Fernández-Merino, M. J., Guardia, L., Paredes, J. I., Villar-Rodil, S., Solís-Fernández, P., Martínez-Alonso, A., & Tascón, J. M. D. (2010). *The Journal of Physical Chemistry C*, 114, 6426-6432.

[29] Schniepp, H. C., Li, J. L., Mc Allister, M. J., Sai, H., Herrera-Alonso, M., Adamson, D. H., Prud'homme, R. K., Car, R., Saville, D. A., & Aksay, I. A. (2006). *The Journal of Physical Chemistry B*, 110, 8535-8539.

[30] Mc Allister, M. J., Li, J. L., Adamson, D. H., Schniepp, H. C., Abdala, A. A., Liu, J., Herrera-Alonso, M., Milius, D. L., Car, R., Prud'homme, R. K., & Aksay, I. A. (2007). *Chemistry of Materials*, 19, 4396-4404.

[31] Steurer, P., Wissert, R., Thomann, R., & Mülhaupt, R. (2009). *Macromolecular Rapid Communications*, 30, 316-327.

[32] Kudin, K. N., Ozbas, B., Schniepp, H. C., Prud'homme, R. K., Aksay, I. A., & Car, R. (2007). *Nano Letters*, 8, 36-41.

[33] Wang, X., Hu, Y., Song, L., Yang, H., Xing, W., & Lu, H. (2011). *Journal of Materials Chemistry*, 21, 4222-4227.

[34] Kang, S. M., Park, S., Kim, D., Park, S. Y., Ruoff, R. S., & Lee, H. (2011). *Advanced Functional Materials*, 21, 108-112.

[35] Etmimi, H. M., Tonge, M. P., & Sanderson, R. D. (2011). *Journal of Polymer Science Part A: Polymer Chemistry*, 49, 1621-1632.

[36] Choi, E. K., Jeon, I. Y., Oh, S. J., & Baek, J. B. (2010). *Journal of Materials Chemistry*, 20, 10936-10942.

[37] Huang, Y., Qin, Y., Zhou, Y., Niu, H., Yu, Z. Z., & Dong, J. Y. (2010). *Chemistry of Materials*, 22, 4096-4102.

[38] Lee, S. H., Dreyer, D. R., An, J., Velamakanni, A., Piner, R. D., Park, S., Zhu, Y., Kim, S. O., Bielawski, C. W., & Ruoff, R. S. (2010). *Macromolecular Rapid Communications*, 31, 281-288.

[39] Lee, S. H., Kim, H. W., Hwang, J. O., Lee, W. J., Kwon, J., Bielawski, C. W., Ruoff, R. S., & Kim, S. O. (2010). *Angewandte Chemie International Edition*, 49, 10084-10088.

[40] Goncalves, G., Marques, P. A. A. P., Barros-Timmons, A., Bdkin, I., Singh, M. K., Emami, N., & Gracio, J. (2010). *Journal of Materials Chemistry*, 20, 9927-9934.

[41] Li, G. L., Liu, G., Li, M., Wan, D., Neoh, K. G., & Kang, E. T. (2010). *The Journal of Physical Chemistry C*, 114, 12742-12748.

[42] Yang, Y., Wang, J., Zhang, J., Liu, J., Yang, X., & Zhao, H. (2009). *Langmuir*, 25, 11808-11814.

[43] Fang, M., Wang, K., Lu, H., Yang, Y., & Nutt, S. (2009). *Journal of Materials Chemistry*, 19, 7098-7105.

[44] Fang, . M., Wang, K., Lu, H., Yang, Y., & Nutt, S. (2010). *Journal of Materials Chemistry*, 20, 1982-1992.

[45] Wang, D., Ye, G., Wang, X., & Wang, X. (2011). *Advanced Materials*, 23, 1122-1125.

[46] Pramoda, K. P., Hussain, H., Koh, H. M., Tan, H. R., & He, C. B. (2010). *Journal of Polymer Science Part A: Polymer Chemistry*, 48, 4262-4267.

[47] Coessens, V., Pintauer, T., & Matyjaszewski, K. (2001). *Progress in Polymer Science*, 26, 337-377.

[48] Bang, J. H., & Suslick, K. S. (2010). *Adv. Mater.*, 22, 1039-1059.

[49] Suslick, K. S., & Price, G. J. (1999). *Annu. Rev. Mater. Sci.*, 29, 295-326.

[50] Zhai, W., Yu, J., & He, J. (2008). *Polymer*, 49, 2430-2434.

[51] Cravotto, G., & Cintas, P. (2010). *Chemistry- A European Journal*, 16, 5246-5259.

[52] Suslick, K. S., & Flannigan, D. J. (2008). *Annual Review of Physical Chemistry*, 59, 659-683.

[53] Xu, H., & Suslick, K. S. (2011). *Journal of the American Chemical Society*, 133, 9148-9151.

[54] Steenackers, M., Gigler, A. M., Zhang, N., Deubel, F., Seifert, M., Hess, L. H., Lim, C. H. Y. X., Loh, K. P., Garrido, J. A., Jordan, R., Stutzmann, M., & Sharp, I. D. (2011). *Journal of the American Chemical Society*, 2011(133), 10490-10498.

[55] Zhang, B., Zhang, Y., Peng, C., Yu, M., Li, L., Deng, B., Hu, P., Fan, C., Li, J., & Huang, Q. (2012). *Nanoscale*, 2012(4), 1742-1748.

[56] Lee, W. H., Suk, J. W., Chou, H., Lee, J., Hao, Y., Wu, Y., Piner, R., Akinwande, D., Kim, K. S., & Ruoff, R. S. (2012). *Nano Letters*.

[57] Veca, L. M., Lu, F., Meziani, M. J., Cao, L., Zhang, P., Qi, G., Qu, L., Shrestha, M., & Sun, Y. P. (2009). *Chemical Communications*, 2565-2567.

[58] Yu, D., & Dai, L. (2009). *The Journal of Physical Chemistry Letters*, 1, 467-470.

[59] Salavagione, H. J., & Martĩnez, G. (2011). *Macromolecules*, 44, 2685-2692.

[60] Zhuang, X. D., Chen, Y., Liu, G., Li, P. P., Zhu, C. X., Kang, E. T., Noeh, K. G., Zhang, B., Zhu, J. H., & Li, Y. X. (2010). *Advanced Materials*, 22, 1731-1735.

[61] Martínez, G., & Millán, J. L. (2004). *Journal of Polymer Science Part A: Polymer Chemistry*, 42, 6052-6060.

[62] Martínez, G. (2006). *Journal of Polymer Science Part A: Polymer Chemistry*, 44, 2476-2486.

[63] Yu, D., Yang, Y., Durstock, M., Baek, J. B., & Dai, L. (2010). *ACS Nano*, 4, 5633-5640.

[64] Choi, . J., Kim, K. j., Kim, B., Lee, H., & Kim, S. (2009). *The Journal of Physical Chemistry C*, 113, 9433-9435.

[65] Strom, T. A., Dillon, E. P., Hamilton, C. E., & Barron, A. R. (2010). *Chemical Communications*, 46, 4097-4099.

[66] Xu, X., Luo, Q., Lv, W., Dong, Y., Lin, Y., Yang, Q., Shen, A., Pang, D., Hu, J., Qin, J., & Li, Z. (2011). *Macromolecular Chemistry and Physics*, 212, 768-773.

[67] He, H., & Gao, C. (2010). *Chemistry of Materials*, 22, 5054-5064.

[68] Lin, Y., Jin, J., & Song, M. (2011). *Journal of Materials Chemistry*, 21, 3455-3461.

[69] Shan, C., Yang, H., Han, D., Zhang, Q., Ivaska, A., & Niu, L. (2009). *Langmuir*, 25, 12030-12033.

[70] Deng, Y., Li, Y., Dai, J., Lang, M., & Huang, X. (2011). *Journal of Polymer Science Part A: Polymer Chemistry*, 49, 1582-1590.

[71] Vuluga, D., Thomassin, J. M., Molenberg, I., Huynen, I., Gilbert, B., Jerome, C., Alexandre, M., & Detrembleur, C. (2011). *Chemical Communications*, 47, 2544-2546.

[72] Shen, B., Zhai, W., Lu, D., Wang, J., & Zheng, W. (2012). *RSC Advances*, 2, 4713-4719.

[73] Duan, Q., Miura, Y., Narumi, A., Shen, X., Sato, S. I., Satoh, T., & Kakuchi, T. (2006). *Journal of Polymer Science Part A: Polymer Chemistry*, 44, 1117-1124.

[74] Scales, C. W., Convertine, A. J., & Mc Cormick, C. L. (2006). *Biomacromolecules*, 7, 1389-1392.

[75] Zhou, N., Lu, L., Zhu, J., Yang, X., Wang, X., Zhu, X., & Zhang, Z. (2007). *Polymer*, 48, 1255-1260.

[76] Segui, F., Qiu, X. P., & Winnik, F. M. (2008). Journal of Polymer Science Part A: Polymer Chemistry ., 46, 314-326.

[77] Meuer, S., Braun, L., & Zentel, R. (2008). *Chemical Communications*, 3166-3168.

[78] Meuer, S., Braun, L., Schilling, T., & Zentel, R. (2009). *Polymer*, 50, 154-160.

[79] Xu, J., Tao, L., Boyer, C., Lowe, A. B., & Davis, T. P. (2010). *Macromolecules*, 44, 299-312.

[80] Liu, J., Tao, L., Yang, W., Li, D., Boyer, C., Wuhrer, R., Braet, F., & Davis, T. P. (2010). *Langmuir*, 26, 10068-10075.

[81] Liu, J., Yang, W., Tao, L., Li, D., Boyer, C., & Davis, T. P. (2010). *Journal of Polymer Science Part A: Polymer Chemistry*, 48, 425-433.

[82] Xu, L. Q., Wang, L., Zhang, B., Lim, C. H., Chen, Y., Neoh, K. G., Kang, E. T., & Fu, G. D. (2011). *Polymer*, 52, 2376-2383.

[83] Qi, X., Pu, K. Y., Li, H., Zhou, X., Wu, S., Fan, Q. L., Liu, B., Boey, F., Huang, W., & Zhang, H. (2010). *Angewandte Chemie International Edition*, 49, 9426-9429.

[84] Qi, X., Pu, K. Y., Zhou, X., Li, H., Liu, B., Boey, F., Huang, W., & Zhang, H. (2010). *Small*, 6, 663-669.

[85] Yang, H., Zhang, Q., Shan, C., Li, F., Han, D., & Niu, L. (2010). *Langmuir*, 26, 6708-6712.

[86] Cheah, K., Simon, G. P., & Forsyth, M. (2001). *Polym. Int.*, 50, 27-36.

[87] Ginzburg, V. V., Gendelman, O. V., & Manevitch, L. I. (2001). *Phys. Rev. Lett.*, 86, 5073.

[88] Zhang, Z., Zhang, J., Chen, P., Zhang, B., He, J., & Hu, G. H. (2006). *Carbon*, 44, 692-698.

[89] Zhou, T. N., Hou, Z. C., Wang, K., Zhang, Q., & Fu, Q. (2011). *Polymers for Advanced Technologies*, 22, 1359-1365.

[90] Lu, L., Zhou, Z., Zhang, Y., Wang, S., & Zhang, Y. (2007). *Carbon*, 45, 2621-2627.

[91] Liang, J., Huang, Y., Zhang, L., Wang, Y., Ma, Y., Guo, T., & Chen, Y. (2009). *Advanced Functional Materials*, 19, 2297-2302.

[92] Rafiee, M. A., Rafiee, J., Wang, Z., Song, H., Yu, Z. Z., & Koratkar, N. (2009). *ACS Nano*, 3, 3884-3890.

[93] Ramanathan, T. A. A., Abdala, Stankovich. S., Dikin, D. A., Herrera, M., Alonso, R. D., Piner, D. H., Adamson, H. C., Schniepp, Chen. X., Ruoff, R. S., Nguyen, S. T., Aksay, I. A., Prud'Homme, R. K., & Brinson, L. C. (2008). *Nat Nano*, 3, 327-331.

[94] Wang, H., Hao, Q., Yang, X., Lu, L., & Wang, X. (2010). ACS Applied Materials & Interfaces,. 2, 821-828.

[95] Zeng, G., Xing, Y., Gao, J., Wang, Z., & Zhang, X. (2010). *Langmuir*, 26, 15022-15026.

[96] Cardinali, M., Valentini, L., & Kenny, J. M. (2011). *The Journal of Physical Chemistry C*, 115, 16652-16656.

[97] Wang, S., Yu, D., Dai, L., Chang, D. W., & Baek, J. B. (2011). ACS Nano, , 5, 6202-6209.